Journal of Microscopy, Vol. 197, Pt 3, March 2000, pp. 274–284.
Received 3 August 1998; accepted 11 June 1999

Analysis of spherical aberration of a water immersion objective: application to specimens with refractive indices 1.33–1.40

D.-S. WAN*, M. RAJADHYAKSHA*† & R. H. WEBB*
**Wellman Laboratory of Photomedicine, Department of Dermatology, Massachusetts General Hospital, Harvard Medical School, Boston, Massachusetts, U.S.A.*
†Lucid Technologies, Henrietta, New York, U.S.A.

Key words. Confocal microscopy, cover slip, image, immersion medium, interferometry, microscopy, spherical aberration, water immersion objective.

Summary

The method of using immersion medium to correct spherical aberration for water immersion objectives when the samples are not water is investigated. Spherical aberration is measured by an interferometer converted from a confocal microscope for samples with different refractive indices. When the proper refractive index of the immersion medium and thickness of cover slip are selected, the measured spherical aberration approaches zero. A theoretical model can be used for prediction of the immersion medium to correct spherical aberration for various samples. Using the thinnest available cover slip (100 μm), the zero spherical aberration condition can be applied to samples with refractive index as high as 1.40. Confocal images in the condition of almost no spherical aberration are included to demonstrate the improvement of axial resolution due to this correction.

Introduction

Background

Confocal microscopes have used standard oil immersion microscope objective lenses that are designed to inspect a thin object under a glass cover slip of standard (170 μm) thickness. However, in confocal microscopy the observation plane is within a medium of refractive index close to that of water, and at a distance down to 2000 μm from the lens, especially for biological applications (Rajadhyaksha *et al*., 1995; Webb, 1996). Therefore there is a discrepancy between the objective's nominal design and its application to confocal microscopy.

Correspondence to: Der-Shen Wan, New Dimension Research, 400 West Cummings Park, Suite 3000, Woburn, MA 01801, U.S.A. Tel: +1 781 933 1165; fax: +1 781 933 1214; e-mail: dswan@newdri.com

Recently, water immersion microscope objectives have been introduced by many manufacturers. Confocal images with water immersion objectives are usually better than those obtained with standard oil immersion objectives, especially for images deep below the cover slip, because of the better match of refractive index between the immersion medium (water) and the specimen. However, information is usually not available to the user about spherical aberration that occurs when the sample has a refractive index different from that of water. In order to solve the problem of spherical aberration, certain water immersion objectives are equipped with correction collars to adjust for thickness variations of the cover slip or for the refractive index change of solute in water (Keller, 1995).

On the other hand, it is possible to use diffraction theory to calculate the point spread function of an oil immersion objective focusing into water (Sheppard & Gu, 1992; Hell *et al*., 1993; Sheppard & Török, 1996). However, for the purpose of calculating spherical aberration we will use a simple ray tracing model in this paper, and the interferometry results show the ray tracing model works very well when we are dealing with the problem of spherical aberration, even with high numerical aperture.

Outline

In this paper we report a method to use water immersion objectives without correction collars to image specimens with refractive indices different from that of water (in the range 1.33–1.40) without generating spherical aberration. Although the microscope objective was designed for using water as immersion medium and imaging a sample under a cover slip with thickness 170 μm, it is possible to eliminate spherical aberration in the confocal image for samples immersed in a medium other than water. The reason is

that the aberration contributed by the last surface of the objective (i.e. the surface adjacent to the immersion medium) can be tuned by varying the refractive index of the immersion medium to match the change of aberration caused by the cover slip when the sample's refractive index is different from that of water.

The principle of using the immersion medium to correct spherical aberration is first demonstrated by interferometry, which measures spherical aberration in the condition of confocal image. Assuming the microscope objective's original design condition is known, a theoretical or ray tracing model is used to find the refractive index of the immersion medium for the correction of spherical aberration. The agreement is good between the refractive indices found by interferometry and by the ray tracing model, which confirms the viability of this method. The possibility for applying this method to oil immersion objectives for imaging specimens with refractive index close to water is also discussed.

In the last part of this paper we show the direct impact of this aberration on confocal images, and demonstrate it by measuring the axial point spread function when the optimum and non-optimum immersion medium are used in confocal microscopy. Confocal images in the condition of almost no spherical aberration are also included to show the improvement of axial resolution.

Origin of spherical aberration

Definition of spherical aberration of the objective

A parallel plate inserted in a convergent beam will introduce spherical aberration (Smith, 1991; p. 99), so the design of a microscope objective considers the cover slip as the last element of the lens. However, in confocal microscopy, the specimen is below the cover slip and the refractive index of the specimen may not be the same as that of water. Once the surface of the cover slip adjacent to the specimen (surface 3 in Fig. 1) introduces aberration different from design (due to the change of refractive index of the specimen), the total aberration of the objective is no longer zero. We show in this paper that the small change in refractive index of the sample will introduce aberration that cannot be neglected.

If we regard the objective as not including the cover slip, then the wave front traced from the side of the observer to the immersion medium actually contains a large amount of spherical aberration. This spherical aberration is called 'the aberration of the objective' in this paper, and is equal (but of opposite sign) to the aberration of the cover slip under the design conditions, where water is the immersion medium and the sample is immersed in water under a cover slip with thickness 170 μm. Finally, because of the difference in refractive indices across the last surface of the objective, the aberration of the objective is a function of the refractive index of the immersion medium.

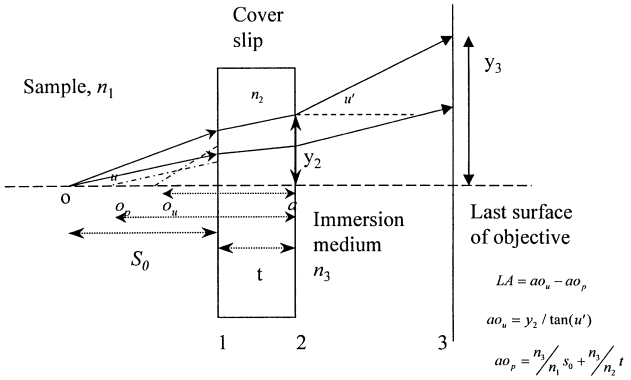

Fig. 1. Ray tracing model: spherical aberration of the cover slip. It shows rays coming from a point source *o* in the sample space and propagating to the space of immersion medium. The virtual sources of these two rays in the immersion medium are two points o_u and o_p. The distance between o_u and o_p is the aberration of the cover slip.

Spherical aberration of the cover slip

As illustrated by Fig. 1, the longitudinal spherical aberration of the cover slip *LA* is expressed as

$$LA = \left[s_0 \sqrt{\frac{n_3^2 - NA^2}{n_1^2 - NA^2}} + t \sqrt{\frac{n_3^2 - NA^2}{n_2^2 - NA^2}} \right] - \left(\frac{n_3}{n_1} s_0 + \frac{n_3}{n_2} t \right). \quad (1)$$

Here s_0 is the distance from a point to be imaged in the specimen space to the cover slip, t is the thickness of the cover slip, and n_1, n_2 and n_3 are refractive indices of specimen, cover slip and immersion medium. *NA* is the numerical aperture of the ray (i.e. $n \sin u$), and the ray tracing direction is from the specimen to the immersion medium. The first part in the square bracket of Eq. (1) is the distance from surface 2 of the cover slip to the virtual image seen in the space of the immersion medium, using the ray with numerical aperture *NA*. The second part in parentheses of Eq. (1) is the same quantity for the paraxial ray ($NA = 0$). The difference between these two quantities defines longitudinal spherical aberration for a ray with numerical aperture *NA*.

The longitudinal spherical aberration shown in Eq. (1) is a negative quantity, and is usually called under-corrected spherical aberration. The amount of under-corrected spherical aberration decreases with the increase of the refractive index of the immersion medium but increases with the increase of thickness of the cover slip and the increase of refractive index of specimen. Figure 2 shows this

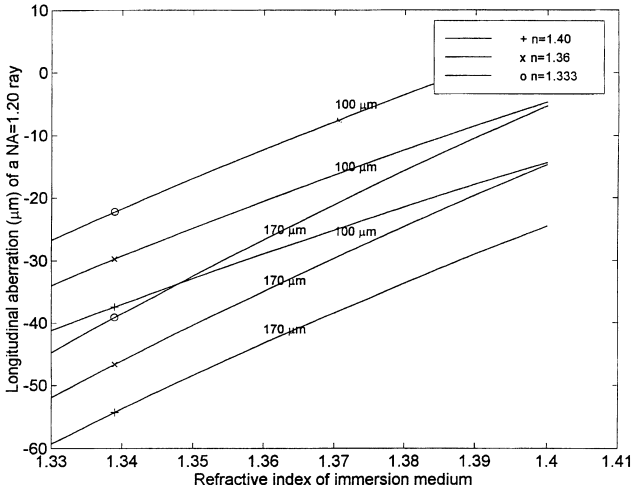

Fig. 2. Aberration of cover slip of thickness 170 μm, and thickness 100 μm, ○: specimen $n = 1.333$, ×: specimen $n = 1.360$, and + specimen $n = 1.40$; thickness of specimen 100 μm.

relationship as a family of lines of the longitudinal aberration of the cover slip vs. the refractive index of the immersion medium for a ray with $NA = 1.2$ calculated by Eq. (1); the thickness of cover slips are 170 μm and 100 μm, respectively.

On the other hand, if the spherical aberration of the ray with the same *NA* traced from the objective is also plotted as the function of refractive index of the immersion medium, the intersection of the aberration of objective and aberration of cover slip will give the condition of zero spherical aberration for this ray. We will find this zero spherical aberration condition first by measuring spherical aberration of the whole system that is combined with objective and cover slip, and then using a ray tracing model to compare with experimental results.

Measuring spherical aberration by interferometry

Interferometry set-up

We used an interferometer to measure the effects of using the immersion medium to correct the spherical aberration. Except in one condition, the wave aberration was measured when the objective was used with a cover slip.

The interferometer was converted from a confocal microscope, so the system aberration was monitored in a condition as similar as possible to the condition of the objective being used in the confocal microscope. The set-up of the Fizeau interferometer used in this experiment is shown in Fig. 3. In this study, we use a Leitz 100× NA = 1.2 water immersion objective as an example to measure the aberration. The samples are gels with different concentrations of scatterers to mimic biological tissue, and the immersion media are sucrose solutions. The refractive indices of the immersion media and gels are measured by a refractometer, with an accuracy of approximately three decimal points. When we do the interferometry test, a 50% reflective surface is put behind the gel as a reflector. The reason for using this reflector is to match the intensity of the test beam with the intensity of the reference beam for the interference purpose. The interferogram is recorded by a CCD camera at the image plane of the microscope pupil, as shown in Fig. 3.

Interferometry results for objective without a cover slip

First, we will show a special case of no cover slip: zero thickness of the cover slip and the same refractive index of

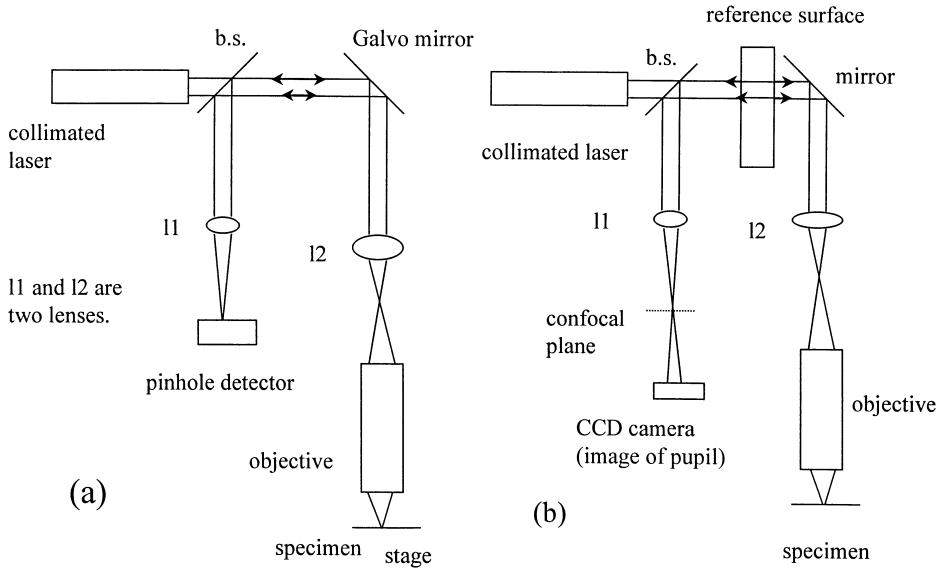

Fig. 3. (a) Schematic diagram of a confocal microscope; (b) a Fizeau interferometer converted from a confocal microscope.

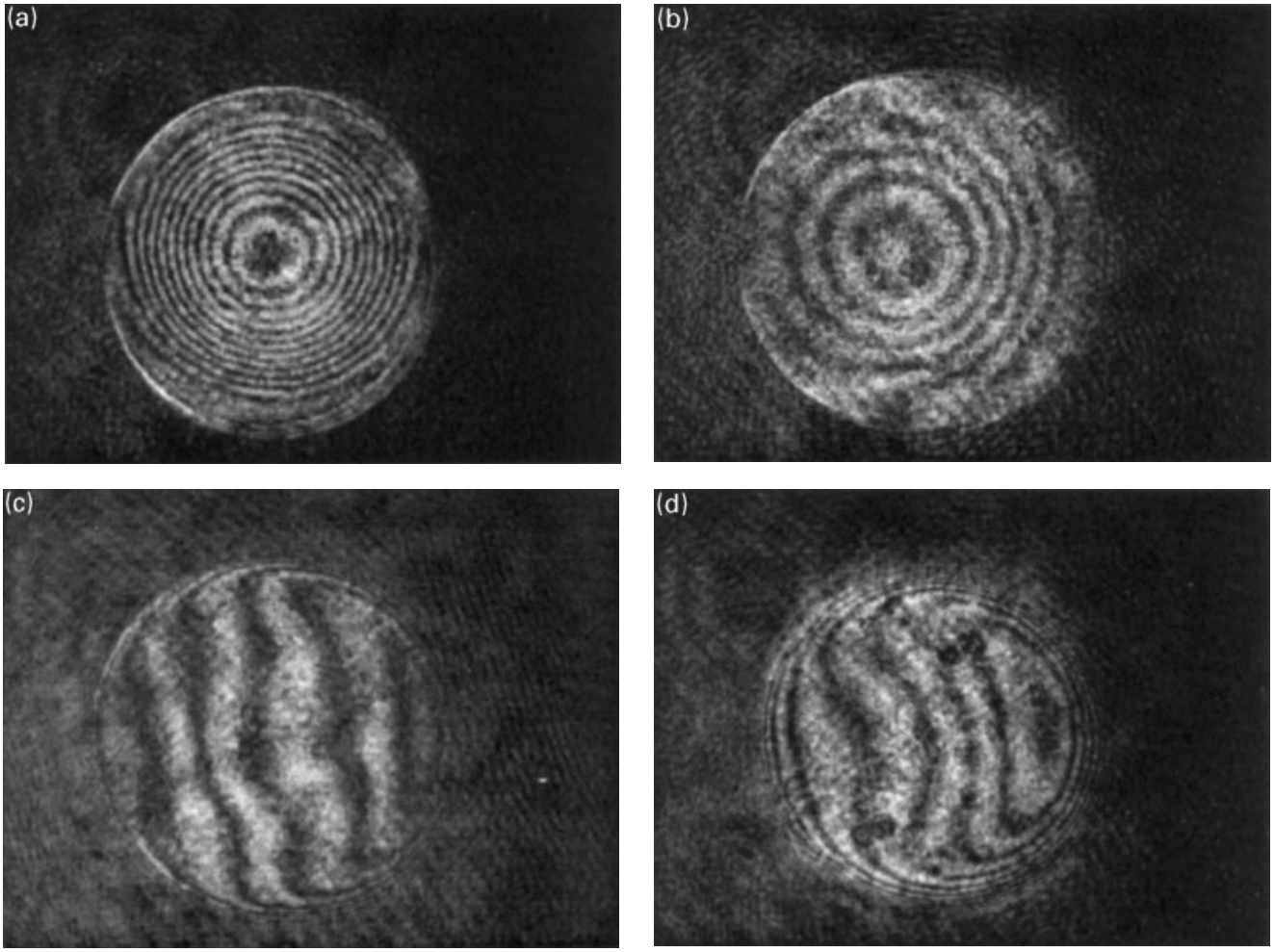

Fig. 4. Interferograms of the objective tested without cover slip and refractive indices of the immersion medium: (a) $n = 1.360$, (b) $n = 1.379$, (c) $n = 1.390$ and (d) $n = 1.410$.

the immersion medium and the sample. This measures the spherical aberration of the objective as defined in the previous section. Figure 4 shows four interferograms of this objective when the refractive indices of the immersion media are 1.360, 1.379, 1.390 and 1.410 and there is no cover slip. For refractive indices of the immersion medium lower than 1.39, the objective generates under-corrected spherical aberration. The aberration approaches zero when the refractive index approaches 1.39, and the aberration becomes overcorrected when the refractive index is above 1.39.

To determine whether the aberration is under-corrected or overcorrected we change the defocus. When the defocus is toward the direction of the objective and the wave aberration near the pupil boundary decreases, the aberration is called under-corrected. Otherwise, it is overcorrected. The interferograms in Fig. 4 indicate that the under-corrected spherical aberration of this objective decreases (shown by straighter fringes) when the refractive index of the immersion medium increases. The variation of aberration of the objective with respect to the refractive index of the immersion medium shows the same trend as the aberration of the cover slip. That is, the under-corrected spherical aberration decreases as the refractive index of the immersion medium increases. This trend implies that it is possible to use the immersion medium to cancel the aberration of the objective with the aberration of the cover slip.

Interferometry results for objective with cover slip

For immersion media with refractive indices not in the range 1.36–1.41, cover slips are included in the system for the interferometry test. For a given specimen (a gel), we use various immersion media with different refractive indices and check where the zero aberration occurs by interferometry.

Figure 5 shows four interferograms for a gel with

refractive index 1.343 when a 145 μm cover slip was used. The reason to choose a gel with refractive index 1.343 is to mimic the refractive index of human epidermis (Tearney *et al.*, 1995). In Fig. 5a and b the refractive indices of the immersion media are 1.333 and 1.350, respectively, and both interferograms show spherical aberration but with opposite sign (under-corrected and overcorrected). The 1.333 immersion has under-corrected aberration and the 1.35 immersion has overcorrected aberration, so it is apparent that the refractive index of the immersion medium generating no spherical aberration occurs between 1.333 and 1.35. Figures 5c and d show interferograms of immersion medium refractive index 1.343, and the straight fringes indicate no aberration. Because in this case the best immersion medium happened to have the same refractive index as the specimen, the specimen thickness will not affect the aberration Eq. (1). The specimen thicknesses in Fig. 5c and d are 80 μm and 20 μm, respectively. Substituting the value 1.343 for n_1 and n_3 in Eq. (1) (and taking the refractive index of the cover slip as 1.515 for the 0.633 μm wavelength), the ray aberration of the objective is found. Zero spherical aberration means that the aberration of the objective is totally balanced by the aberration of the cover slip.

By similar procedures, the refractive indices of the immersion media to correct spherical aberration for samples with refractive index 1.359, 1.354 and 1.333 are found (with 145 μm cover slip). The results are listed in Table 1.

When the refractive index of the sample is further increased, we use a thinner cover slip so that we can use an immersion medium with refractive index higher than that of water. Figure 6 shows interferograms of no spherical aberration for two specimens with refractive indices 1.398 and 1.419, and sample thickness 115 μm and 87 μm, respectively. The thickness of the cover slip is 103 μm. The corresponding refractive indices of the immersion media to eliminate the spherical aberration are 1.335 and 1.337.

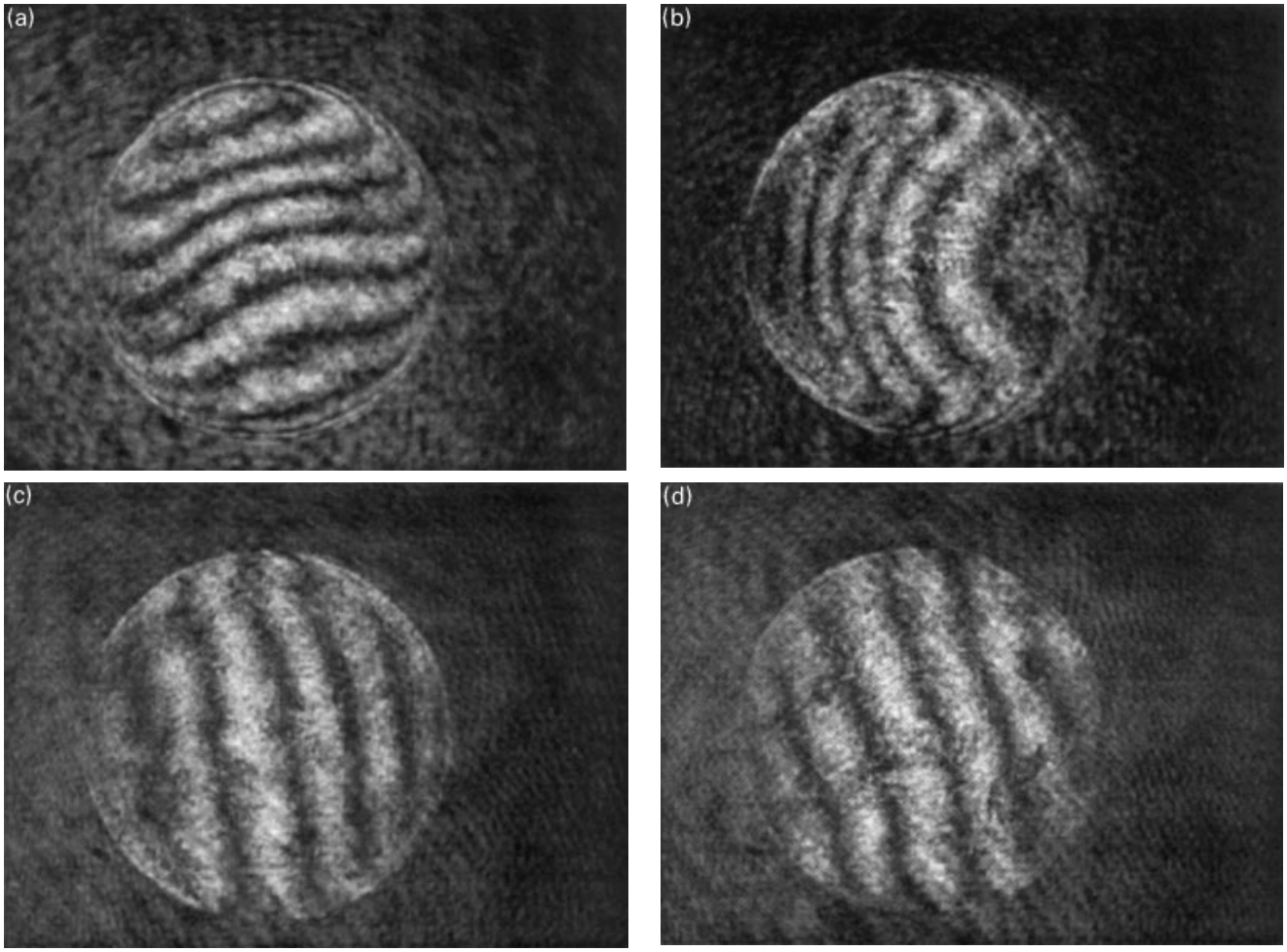

Fig. 5. Interferograms of gel with refractive index 1.343, and immersion medium refractive index (a) $n = 1.33$ (water), (b) $n = 1.35$, (c) $n = 1.343$, gel thickness 80 μm, (d) $n = 1.343$ gel thickness 20 μm.

Table 1. Refractive indices of the immersion media to correct spherical aberration and the conditions (refractive indices of specimens, thickness of specimens and thickness of cover slips) to find these values.

Refractive index of immersion medium		Working distance (μm)	Refractive index of specimen	Specimen thickness (μm)	Cover slip thickness (μm)
Ray tracing	Interferometry				
1.3327	1.335	98.9	1.398	115	103
1.3366	1.337	127.2	1.419	87	103
1.3347	1.340	97.2	1.359	76	145
1.3409	1.342	123.1	1.354	50	145
1.3465	1.343	73.1	1.343	100	145
1.3479	1.347	108.2	1.379	105	103
1.3484	1.348	143.0	1.333	32	143

Ray tracing model for the prediction of immersion medium to correct spherical aberration

Model

As shown in the previous section, the refractive index of the immersion medium can be found by interferometry test. A ray tracing model can also be used for the prediction of the refractive index of the immersion medium to correct spherical aberration provided that the last surface of the objective is plane. In the objective's original design or in any condition of zero spherical aberration found by interferometry, the objective's aberration is equal to the aberration of the cover slip, but if the objective's last surface is plane the ray height on the last surface of objective can also be found. The following two equations show ray heights traced from a point in the space of the sample to the last surface of the objective as notations defined in Fig. 1.

$$y_2 = s_0 \frac{NA}{\sqrt{n_1^2 - NA^2}} + t \frac{NA}{\sqrt{n_2^2 - NA^2}}, \tag{2}$$

and

$$y_3 = y_2 + s_1 \frac{NA}{\sqrt{n_3^2 - NA^2}}. \tag{3}$$

Here NA (i.e. $n \sin u$) is used to specify a ray because NA is unchanged when the ray is refracted by a plane surface, and the maximum NA of all rays is the objective's numerical aperture NA. From the original design conditions of the objective ($s_0 = 0$, $t = 170\,\mu\text{m}$, $s_1 = 150\,\mu\text{m}$, $n_3 = n_1 = 1.333$, and $n_2 = 1.515$ for this Leitz $100\times$ NA $= 1.2$ lens), we calculated the ray heights y_3 in mm on

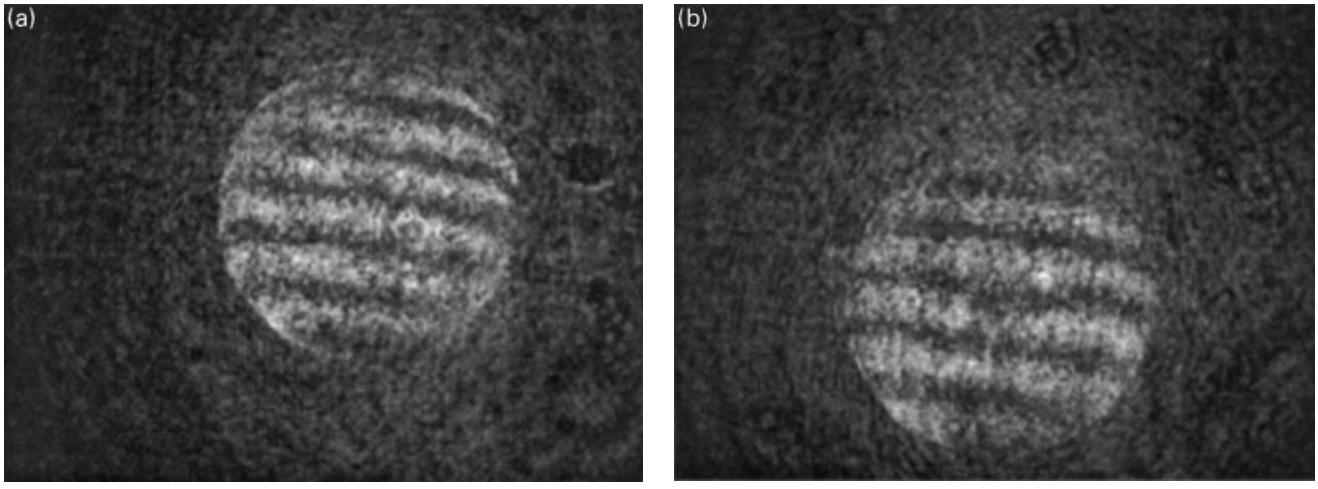

Fig. 6. Interferograms showing no spherical aberration for specimens with higher refractive indices, (a) specimen $n = 1.398$, thickness 110 μm, cover slip 103 μm, (b) specimen $n = 1.419$, thickness 87 μm, cover slip 103 μm.

the last surface. These ray heights are 0.0225, 0.0454, 0.0690, 0.0937, 0.1201, 0.1489, 0.1811, 0.2183, 0.2628, 0.3196, 0.3987 and 0.5307, respectively, with the numerical aperture increased from 0.1 to 1.2 by an interval of 0.1.

The ray heights y_3 listed above are unchanged for rays specified by their numerical apertures (*NA*). It is explained as follows. First, from a point O' in the confocal plane in Fig. 3, rays can also be traced toward the objective lens, where point O' is the conjugate of the point O in Fig. 1 used to calculate y_3 in the design condition. These rays (traced from O') reaching the last surface of the objective have the same heights as rays with the same *NA* traced from point O toward objective because of conjugate relation. It is obvious that the ray heights on the last surface of the objective will not be affected by the refractive index of the immersion medium n_3 and the refractive index of the sample provided that rays are traced from a fixed point O' in the confocal plane. However, point O' and point O are exact conjugate points only in the condition of zero spherical aberration. We can use this fact to predict the immersion medium to correct spherical aberration for different specimens for a specific ray by tracing this ray from point O to the last surface of the objective. Given the refractive index of the sample and its thickness, the refractive index of the immersion medium and working distance s_1 are solved by Eqs (2) and (3) for the condition of zero spherical aberration.

Solution to correct spherical aberration of whole system

Table 1 lists the refractive index of the immersion medium needed to correct spherical aberration in different conditions, as the refractive indices of samples are varied from 1.333 to 1.419. Ray tracing solutions are found by selecting y_3 of the marginal ray ($NA = 1.2$) and y_3 of a paraxial ray ($NA = 0.1$) necessary to correct spherical aberration of the marginal ray, and the solutions are listed in the first column. By comparing ray tracing results with refractive indices of the immersion medium found by interferometry in the second column of Table 1, good agreements are seen (the largest difference in refractive indices predicted and found by interferometry is less than 0.004). This fact implies that this simple ray tracing model is sufficient to describe the effects of correcting spherical aberration by choice of the immersion medium and cover slip.

Discussion

Comparison of ray tracing data with experiment results

The small difference in refractive index of the immersion medium found by ray tracing model and interferometry is mainly due to the measuring uncertainty of the refractive index. However, strictly speaking, the correction of spherical aberration of the marginal ray is not equivalent to zero wave front aberration, which is monitored by the interferometry test. For instance, in the case of correction of spherical aberration of the marginal ray, there is still a small amount of wave aberration expressed by the primary wave aberration coefficient W_{040} (i.e. the wave aberration is expressed as $W(r) = W_{040}r^4$, where r is the normalized radius in exit pupil). The radius of the corresponding spot size is

$$\frac{8}{3\sqrt{3}} W_{040}/NA,$$

which is caused by aberration of rays other than the marginal ray. The ray tracing model can estimate the spot size by calculating the transverse spherical aberration (*TA*) as shown here:

$$TA = y_3 - s_1 \frac{NA}{\sqrt{n_3^2 - NA^2}} - t \frac{NA}{\sqrt{n_2^2 - NA^2}} - s_0 \frac{NA}{\sqrt{n_1^2 - NA^2}}. \quad (4)$$

For example, using the data of sample refractive index 1.343 shown in Table 1, the maximum spot size found by Eq. (4) is 0.67 μm. The diffraction limited spot size, $0.61\lambda/NA$, is 0.32 μm for (NA = 1.2). In order to further reduce the spot size, we can eliminate the spherical aberration of an intermediate ray. If we select the ray $NA = 1.18$, then the refractive index of the immersion medium is 1.3478 and the maximum spot size is reduced to 0.55 μm, approaching the minimum circle, W_{040}/NA. However, compared with the marginal ray solution ($n_3 = 1.3465$), the difference in refractive index is 0.0013, which is difficult to measure.

In order to match the ray tracing model more closely to the interferometry results, both the accuracy in measuring refractive index and wave aberration need to be improved. Very accurate measurement of spherical aberration is usually achieved by phase shift interferometers (Greivenkamp & Bruning, 1992, p. 501), but that is difficult to implement in the environment of confocal microscopy because of the very strict stability requirement in the phase shift interferometer. Measurement of the refractive index of a liquid with convenient devices like saccarimeters, at their best, generally restricts accuracy to one to two units in the fourth place. Despite the difficulty for further improvement in measuring accuracy, the comparison in Table 1 shows that the ray tracing model is a very good approximation to predict the refractive index of the immersion medium for correction of spherical aberration.

Interferometry tests indicate the real conditions when the system was measured without aberration, and the results can also be used to calculate the longitudinal spherical aberration if the small difference between ray tracing and wave aberration mentioned in the previous paragraph is

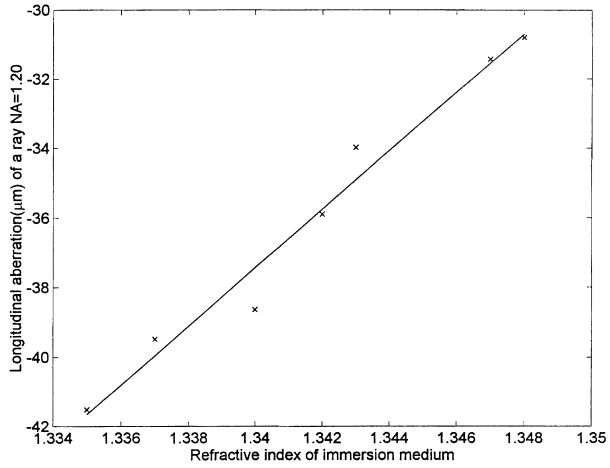

Fig. 7. Longitudinal spherical aberration of the objective represented by the NA = 1.2 ray, ×: data found by interferometry test, solid line: least squares fitting.

neglected. Figure 7 shows a straight line fit by longitudinal spherical aberration of the objective which is calculated by Eq. (1) with refractive indices of the immersion media found by interferometry shown in Table 1. The fit agrees well with experiment, so the difference of the refractive indices of the immersion medium predicted by this model and found by experiments seems due to the experimental uncertainty.

The aberration curve of the objective fitted by the data is useful when the last surface of the objective is not a plane. In this case, the refractive index of the immersion medium cannot be predicted by the ray tracing model. Here, the aberration of the objective is found by interferometry as a function of the refractive index of the immersion medium. The refractive index n_3 of the immersion medium to correct the spherical aberration will be found by equating the aberration of the cover slip to the aberration of the objective, i.e.

$$an_3 + b = \left[s_0 \sqrt{\frac{n_3^2 - NA^2}{n_1^2 - NA^2}} + t \sqrt{\frac{n_3^2 - NA^2}{n_2^2 - NA^2}} \right] - \left(\frac{n_3}{n_1} s_0 + \frac{n_3}{n_2} t \right), \quad (5)$$

where $an_3 + b$ is the experimental straight line in Fig. 7.

Tolerance analysis

The transverse spherical aberration (*TA*) in the object plane of the whole system is shown by Eq. (4). The *TA* can be used to estimate the change of spot size due to the deviation from design values such as refractive indices of the immersion medium and sample, and thickness of sample. In the case of sample refractive index 1.343 (condition shown in Table 1), the transverse spherical aberration of the marginal ray will be as large as 7.5 μm if water instead of refractive index 1.3465 is used as the immersion medium. Similarly, if water is the sample, using refractive index 1.3465 as the immersion medium, the transverse spherical aberration of the marginal ray is 7.7 μm. In both analyses the working distance is kept as the design value.

In summary, spherical aberration of the system is very sensitive to the change of refractive indices in the immersion medium and sample but less sensitive to the change of sample thickness. This property is useful because confocal images are usually focused at different depths.

It can also be seen from the interferograms (Figs 4 and 5) that a small change of refractive index causes a perceptible change of wave aberration. If sucrose solution is used as the immersion medium, it is necessary to measure the refractive index each time before using it since its refractive index may change over several days.

As shown in the previous section, there are cases when the refractive index to correct the spherical aberration is equal to the refractive index of the sample, and under these conditions the thickness of the sample has no effect on spherical aberration at all. For three common cover slips, 170 μm, 145 μm, and 100 μm, the corresponding refractive indices of specimens (also of the immersion media of objective) are found as 1.333, 1.3445 and 1.361, respectively, by the theoretical model. The latter two cases are also found by interferometry, and the corresponding refractive indices are 1.343 (Fig. 5c, d) and 1.359 (Fig. 8). Using the experimental straight line shown in Fig. 7 and solving Eq. (5), the prediction of the refractive index of the immersion medium to eliminate spherical aberration by using 170 μm cover slip is 1.334. The theoretical value 1.333 is a check of the accuracy of the experimental data.

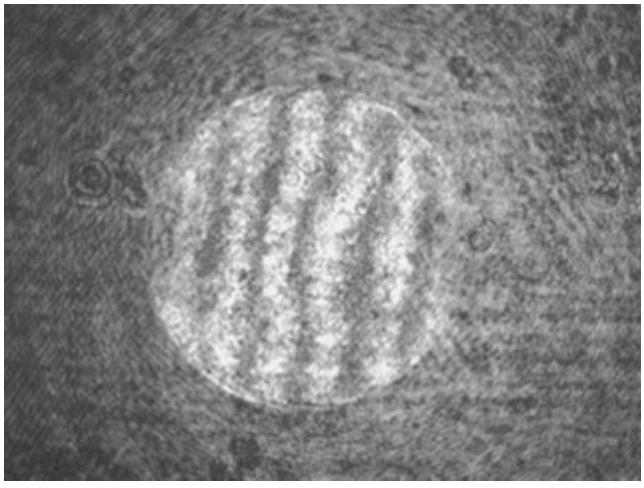

Fig. 8. Interferogram of immersion media of objective and specimen having the same refractive index 1.359, and cover slip thickness 105 μm.

Table 2. Conditions to correct spherical aberration for a 98 × NA = 1.3 oil immersion objective to image samples with refractive index 1.333.

Refractive index of immersion medium	2.179	1.823	1.647	1.585
Thickness of cover slip (μm)	145	100	100	100
Thickness of sample (μm)	30	30	50	30
NA of the ray corrected without spherical aberration	1.3	1.3	0.9	0.9
Working distance (μm)	188	212	228	184

Conditions of implementing the interferometry test

If interferometry is used to monitor the aberration of the confocal system, we need to take care of various factors that affect the contrast in interferometry, such as vibration isolation, coherence length of the laser, and intensity match between reference and test beam. Fringes must have good contrast, so the tester can see the change of the aberration near the boundary of the objective's pupil. That is the most sensitive part to see the variation of aberration. For the same reason, in order to find a clear boundary, especially for high numerical aperture objectives, interferograms should be recorded at the image plane of the microscope pupil (which is found by shining light into the objective from the side of sample). The aberration of the other lenses in the interferometer, such as lens 2 shown in Fig. 3(b), usually can be neglected, because the small beam diameter makes the working f/# very large (i.e. very small NA). In this experiment, we determine whether aberration exists by checking the straightness of fringes.

The determination of thickness in our measurements is found by focusing a laser beam on the interface between the cover slip and the specimen, and again on the interface between the specimen and the reflector, and this is checked visually for minimum spot size in the confocal plane (Fig. 3). The real thickness is the difference from the readings of the actuator for these two focal positions multiplied by the ratio of refractive index of the specimen to that of the cover slip. As shown in the previous section, the aberration is not strongly dependent on the thickness of the sample.

Using oil immersion objectives to image specimens with refractive index near water without spherical aberration

The method developed in this paper can be applied to many other objectives, provided that the refractive index of the immersion medium and working distance found are reasonable, i.e. the refractive index is not either too high or too low and the working distance is positive. Here we use an oil immersion 98× NA = 1.3 objective (Laikin, 1995; p. 130) as an example. From the lens data, we know the nominal working distance is 140 μm, and it has no spherical aberration when immersed in oil. Then we can find the fixed ray pattern on the last surface (a flat surface). Assuming the sample immersed in water, the working distance and the immersion medium to correct spherical aberration are found by matching ray height on the last surface of the objective, and Table 2 lists some results.

The data in Table 2 show that in order to correct the aberration of the whole system, the immersion medium causes overcorrected spherical aberration in the objective rather than under-corrected spherical aberration, as in a water immersion objective. This is due to the fact that the refractive index of the immersion medium is higher than that of cover slip. In this case, a higher refractive index of the immersion medium increases the overcorrected spherical aberration, and a thicker cover slip also increases the overcorrected spherical aberration. Table 2 shows that if the aberration of the marginal ray is corrected, the refractive indices found for the immersion media are 1.823 and 2.179 for 100 μm and 145 μm cover slips and the sample thickness is 30 μm. These high refractive indices are not practical. If the aperture of the objective is stopped down to NA = 0.9, the refractive indices of the immersion media to correct the aberration are 1.5847 and 1.647 for sample thickness 30 μm and 50 μm, respectively, and the cover slip thickness is 100 μm. If the thickness of the sample is increased, the refractive index of the immersion medium to correct the spherical aberration will increase too. In order to get available immersion media to correct the spherical aberration, the stop of the objective must be reduced further.

The effect of spherical aberration on axial point spread function and confocal images

The aberration of the microscope changes the point spread function of the microscope. Figure 9 shows the axial point spread function of this objective in a confocal microscope in the condition of the specimen with refractive index 1.343 and thickness 100 μm, used with 145 μm cover slip, and the pinhole diameter is 75 μm. (3.4 times the diffraction-limited spot). The right-hand plot is for immersion medium refractive index 1.343, which is the case without aberration as indicated by Fig. 5c. The FWHM (full width half maximum) of the axial point spread function is 0.81 μm. The diffraction limited FWHM of the axial point spread function is FWHM = (Webb, 1996), which equals 0.74 μm, where $n = 1.343$, $\lambda = 0.6328$ μm, and NA = 1.2. Because

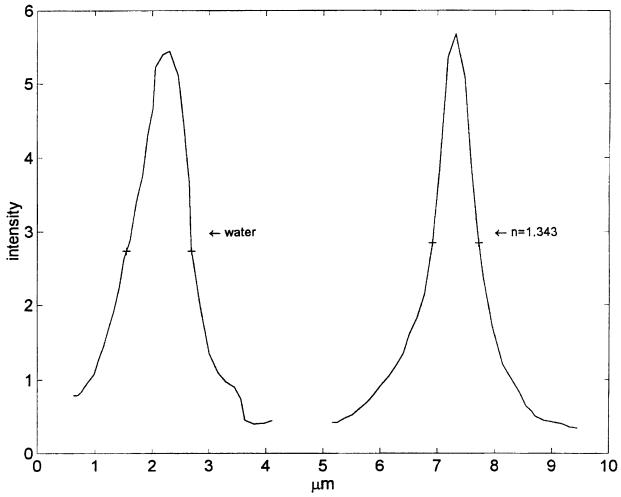

Fig. 9. Axial point spread function of the microscope by using 145 μm cover slip for a specimen with refractive index 1.343, thickness 100 μm, right hand plot: immersion medium $n = 1.343$, FWHM 0.81 μm, and left-hand plot: immersion medium water, FWHM 1.15 μm.

the FWHM of the axial point spread function measured here is very close to the diffraction limited prediction, it confirms once again that there is almost no aberration in this case. The left-hand plot in Fig. 9 is for water as the immersion medium, and the corresponding interferogram in Fig. 5a shows the fourth-order spherical aberration 2.70 μm which is found by fitting the digitized interferogram by Zernike polynomials (Freniere *et al.*, 1981). For such an amount of aberration, the FWHM of the axial point spread function measured is 1.15 μm (Fig. 9).

Finally, confocal images are included to demonstrate the improvement of axial resolution by reducing spherical aberration. The confocal microscope is set as shown in Fig. 3a with functions of horizontal and vertical scanning, and the objective is a Lomo water immersion lens with NA = 0.9 and working distance 1.5 mm. This objective is special for its long working distance, but it has large spherical aberration if used for objects immersed in water without a cover slip. The spherical aberration of this microscope can be reduced dramatically when the refractive index of the immersion medium is 1.34 and the thickness of the cover slip is 100 μm for samples immersed in water. The FWHM of axial point spread function is 1.5 μm compared with 1.3 μm of the diffraction limit resolution.

The samples are human cheek cells, and Figs 10 and 11 are confocal images in horizontal section and vertical section, respectively. In Fig. 11, from top to bottom the three bright lines are images of the first surface and the second surface of the cover slip and the front surface of the Petri dish. It is clear that the image of the front surface of the Petri dish is sharper than the images of cover slip surfaces. That is because spherical aberration is eliminated in the

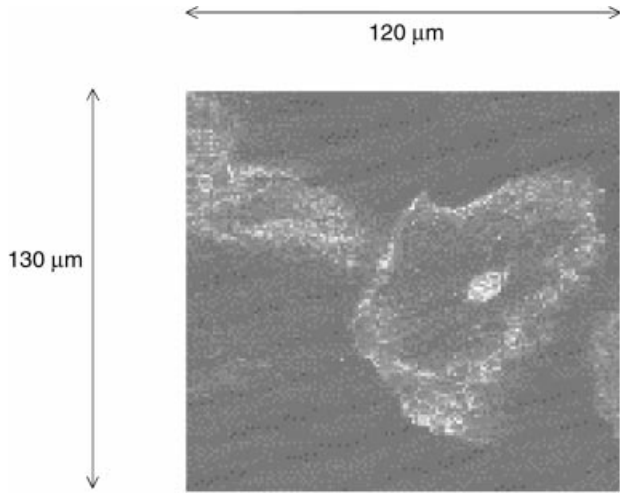

Fig. 10. Confocal image of human cheek cells in horizontal section.

sample space, not on the surface of the cover slip. With spherical aberration reduced, the membrane of the cell in the vertical section can be seen very clearly. The section ability is good as we see that one cell sits atop the other cell in the vertical section image.

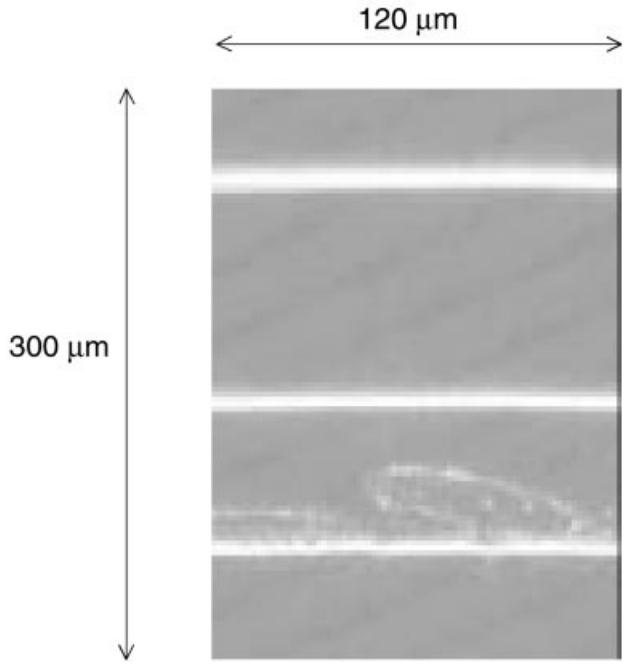

Fig. 11. Confocal image of human cheek cells in vertical section. Three bright lines from top to bottom are front and rear surfaces of the cover slip, and front surface of the Petri dish. With spherical aberration reduced, cell membrane can be seen very clearly. 300 μm is the scanning distance; the real thickness will be modified by refractive index ratio (see text).

Table 3. Condition of zero spherical aberration for a Leitz 100×NA = 1.2 water immersion objective, sample thickness 100 μm.

Thickness of cover slip (μm)	Refractive indices of samples	Refractive indices of the immersion media
170	1.333	1.333*
145	1.333	1.3633
	1.3445	1.3445*
	1.350	1.3374
	1.354	1.333
105	1.333	1.3971
	1.34	1.3856
	1.35	1.3724
	1.3611	1.3611*
	1.37	1.3538
	1.38	1.3470
	1.39	1.3413
	1.40	1.3366
	1.408	1.3333
0	1.3926	1.3926*

* representing conditions independent of sample thickness.

Summary of analysis

As an example, Table 3 lists for three common cover slips (170 μm, 145 μm and 100 μm) and for no cover slip, the conditions of zero spherical aberration of the marginal ray in the whole system (predicted by the ray tracing model) for this 100×NA = 1.2 objective. Here the thickness of the sample is 100 μm, but under conditions where the refractive indices of the specimen and the immersion medium are the same there is no dependence on sample thickness. One of these conditions is the refractive index of the immersion medium and of the sample is 1.3445 when 145 μm cover slip is used. Since this refractive index is very close to that of human epidermis, it should have useful applications for confocal microscopy in human skin.

Conclusion

We have proposed a method for using immersion medium refractive index and cover slip thickness to correct spherical aberration, and have confirmed it by interferometry. This method can help the microscopist to find applications that are not restricted to the objective's original design. In this example, we show the possibility of eliminating spherical aberration for specimens with refractive indices from 1.33 to higher than 1.40 and for specimen thickness thicker than 100 μm, even though this objective was designed for water only.

The analysis presented in this paper can be applied to any general application of confocal imaging of living tissue. For a given objective lens and tissue refractive index, we can determine optimum immersion medium refractive index and cover slip thickness that will minimize spherical aberration (Table 3). This allows us to improve resolution and contrast.

Acknowledgements

We appreciate useful discussions with James M. Zavislan of Lucid Technologies and Charles Lin of Wellman Lab, Massachusetts General Hospital. We also very much appreciate the referees' valuable opinions, especially about the difference in marginal ray aberration and wave aberration. This research was funded by Lucid Technologies and by DE-FG02-91ER61229 from the Office of Health and Environmental Research of the Department of Energy.

References

Freniere, E.R., Toler, O.E. & Race, R. (1981) Interferogram evaluation program for the HP-9825A calculator. *Opt. Eng.* **20**, 253–255.

Greivenkamp, J.E. & Bruning, J.H. (1992) Phase shifting interferometry. *Optical Shop Testing* (ed. D. Malacara), pp. 501–598. Wiley, New York.

Hell, S., Reiner, G., Cremer, C. & Steltzer, E.H.K. (1993) Aberration in confocal fluorescence microscopy induced by mismatches in refractive index. *J. Microsc*, **169**, 391–405.

Keller, H.E. (1995) Objective lenses for confocal microscopy. *Handbook of Biological Confocal Microscopy* (ed. J. B. Pawley), pp. 115–116. Plenum Press, New York.

Laikin, M. (1995) *Lens Design*. Marcel Dekker, New York.

Rajadhyaksha, M., Grossman, M., Esterwitz, D., Webb, R.H. & Anderson, R.H. (1995) *In vivo* confocal scanning laser microscopy of human skin: melanin provides strong contrast. *J. Invest. Dermatol.* **104**, 946–952.

Sheppard, C.J.R. & Gu, M. (1992) Axial imaging through an aberrating layer of water in confocal microscopy. *Opt. Commun.* **88**, 180–190.

Sheppard, C.J.R. & Török, P. (1996) Effects of specimen refractive index on confocal imaging. *J. Microsc.* **185**, 366–374.

Smith, W. (1991) *Modern Optical Engineering*. McGraw-Hill, New York.

Tearney, G.J., Brezinski, M.E., Southern, J.F., Bouma, B.E., Hee, M.R. & Fujimoto, J.G. (1995) Determination of the refractive index of highly scattering human tissue by optical coherence tomography. *Opt. Lett.* **20**, 2258–2260.

Webb, R.H. (1996) Confocal optical microscopy. *Rep. Prog. Phys.* **59**, 427–471.